Supporting Information

Computational Details

The density functional theory as implemented using the Vienna *ab initio* simulation package (VASP, Version: 5.4.4)[1]. The exchange–correlation potential was based on the Perdew–Burke–Ernzerhof (PBE) functional by using the projected augmented wave (PAW) method with the generalized gradient approximation (GGA)[2]. The energy cutoff was set as 520 eV. All the positions of atoms were fully relaxed until the forces on each atom were less than 0.01 eV Å^{-1}. The $2 \times 2 \times 1$ k-mesh were used to integrate the Brillouin zones for the surface (supercell) slab model (Monkhorst–Pack algorithm). The DFT+U method was used where mentioned. The Hubbard U is applied to the Fe-d orbitals (U=5.3 eV). The van der Waals interactions were described via the DFT-D3 method proposed by Grimme[3], which has been shown to accurately describe the chemisorption and physisorption properties of layered materials. The periodic replicas were decoupled in a vacuum region of about 20 Å.

Following Nørskov's strategy[4, 5], the binding energies of OCH$_3$, OCH$_2$OH, HCOO are calculated through

$$\Delta E(\text{OCH}_3) = E(\text{sub/OCH}_3) - [E(\text{sub}) + E(\text{CH}_3\text{OH}) - E(\text{H}_2)/2]$$

$$\Delta E(\text{OCH}_2\text{OH}) = E(\text{sub/OCH}_2\text{OH}) - [E(\text{sub}) + E(\text{HOCH}_2\text{OH}) - E(\text{H}_2)/2]$$

$$\Delta E(\text{HCOO}) = E(\text{sub/HCOO}) - [E(\text{sub}) + E(\text{HCOOH}) - E(\text{H}_2)/2]$$

where $E(\text{sub/OCH}_3)$, $E(\text{sub/OCH}_2\text{OH})$ and $E(\text{sub/HCOO})$ are the total energies of OCH$_3$, OCH$_2$OH and HCOO groups on the substrate, respectively; $\Delta E(\text{sub})$, $E(\text{CH}_3\text{OH})$, $E(\text{HOCH}_2\text{OH})$, $E(\text{HCOOH})$ and $E(\text{H}_2)$ denote the total energies of bare substrate, CH$_3$OH, HOCH$_2$OH, HCOOH and gas H$_2$, respectively.

The adsorption energies for CH$_3$OH, HCOOH and HCOOOH on the substrate were

Corresponding author. E-mail address: zhmiao@ahu.edu.cn

described as:

$$\Delta E(CH_3OH) = E(sub/CH_3OH) - [E(sub) + E(CH_3OH)]$$

$$\Delta E(HCOOH) = E(sub/HCOOH) - [E(sub) + E(HCOOH)]$$

$$\Delta E(HCOOOH) = E(sub/HCOOOH) - [E(sub) + E(H_2CO_3)]$$

Where $E(sub/CH_3OH)$, $E(HCOOH)$ and $E(sub/HCOOOH)$ are the total energies of CH_3OH, HCOOH and HCOOOH groups on the substrate, respectively; $E(sub)$, $E(CH_3OH)$, $E(HCOOH)$ and $E(sub/H_2CO_3)$ denote the total energies of the substrate, CH_3OH, HCOOH and H_2CO_3, respectively.

For gas-phase species, the standard ideal-gas method was used to calculate the free energy. Computational hydrogen electrode (CHE) model was used to calculate the Gibbs free energy change of the elementary reactions[6]. At electrode potential U = 0 V (*vs*. reversible hydrogen electrode), the free energy can be calculated by $\Delta G = \Delta E - T\Delta S + \Delta ZPE$. ΔE is reaction energy of hydrogenation. $T\Delta S$ is the gas-phase entropy contribution at 298 K. ΔZPE is the zero-point energy correction.

Figures
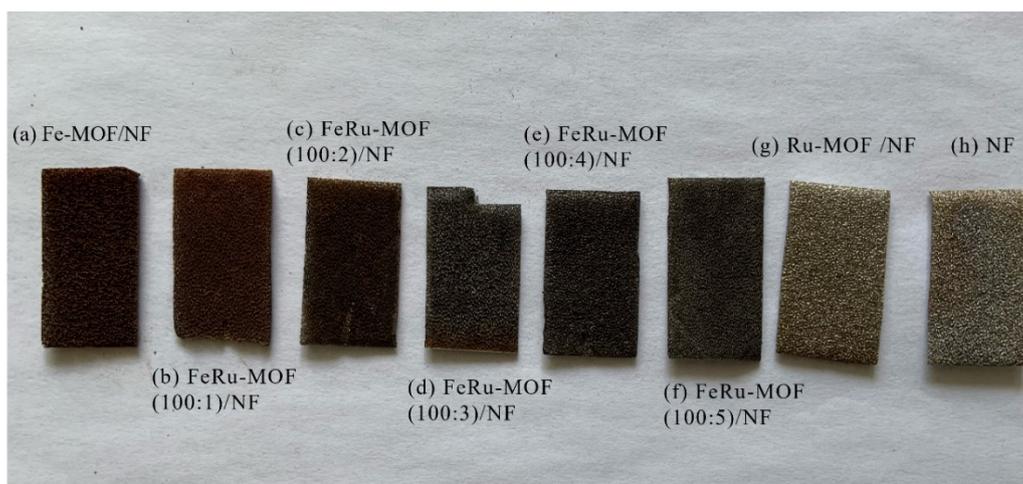
Figure S1. The photograph of (a) Fe-MOF/NF, (b) FeRu-MOF (100:1)/NF, (c)FeRu-MOF (100:2)/NF, (d) FeRu-MOF (100:3)/NF, (e) FeRu-MOF (100:4)/NF, (f) FeRu-MOF (100:5)/NF, (g) Ru-MOF/NF and (h) NF.
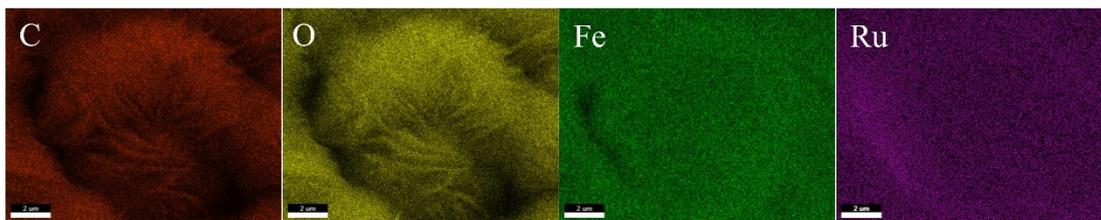
Figure S2. Area SEM-EDX elemental mapping images for C, O, Fe, and Ru of FeRu-MOF (100:3)/NF.

Element	Weight %	Atomic %	Error%
C K	36.86	47.51	6.57
O K	50.84	49.20	8.82
RuL	0.90	0.14	4.36
FeK	11.40	3.16	1.99

Lsec: 286.7   0 Cnts   0.000 keV   Det: Apollo X-SDD
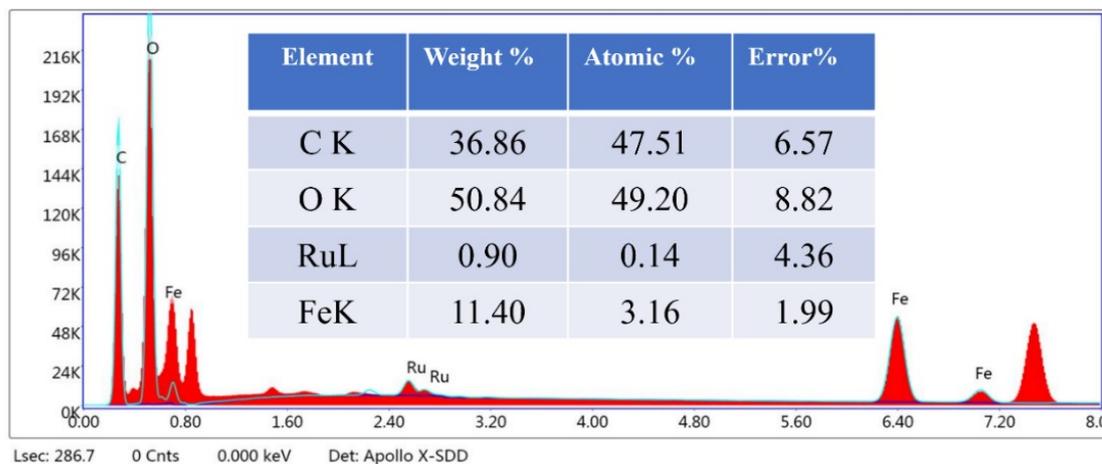
Figure S3. EDX spectrum of FeRu-MOF (100:3)/NF nanosheets.
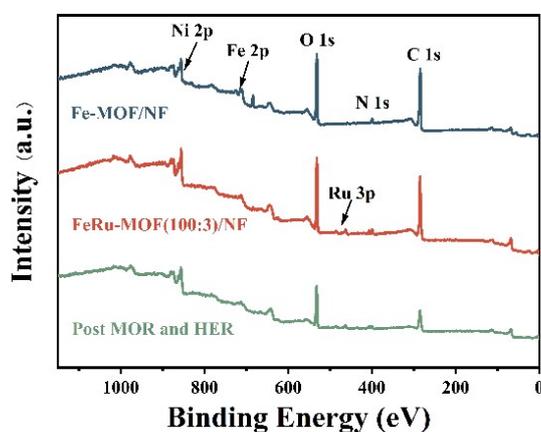
Figure S4. The XPS survey spectrum of the Fe-MOF, FeRu-MOF (100:3) and post MOR and HER FeRu-MOF (100:3) nanosheets.
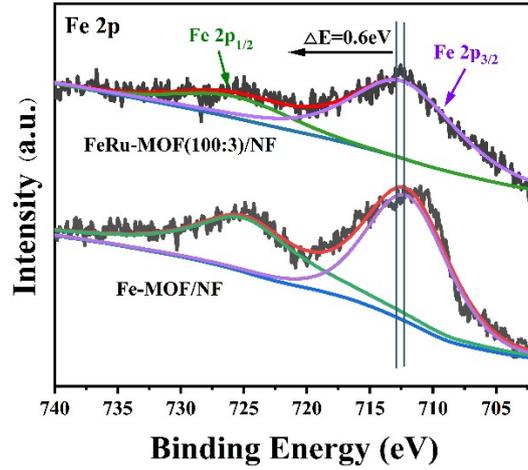
Figure S5. High-resolution Fe 2p XPS spectra of Fe-MOF nanosheets and FeRu-MOF (100:3) nanosheets.
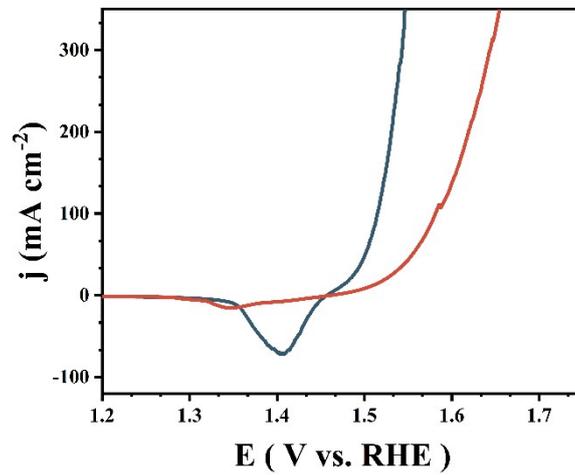
Figure S6. LSV curves for Fe-MOF/NF and FeRu-MOF (100:3)/NF in 1.0 M KOH solution.
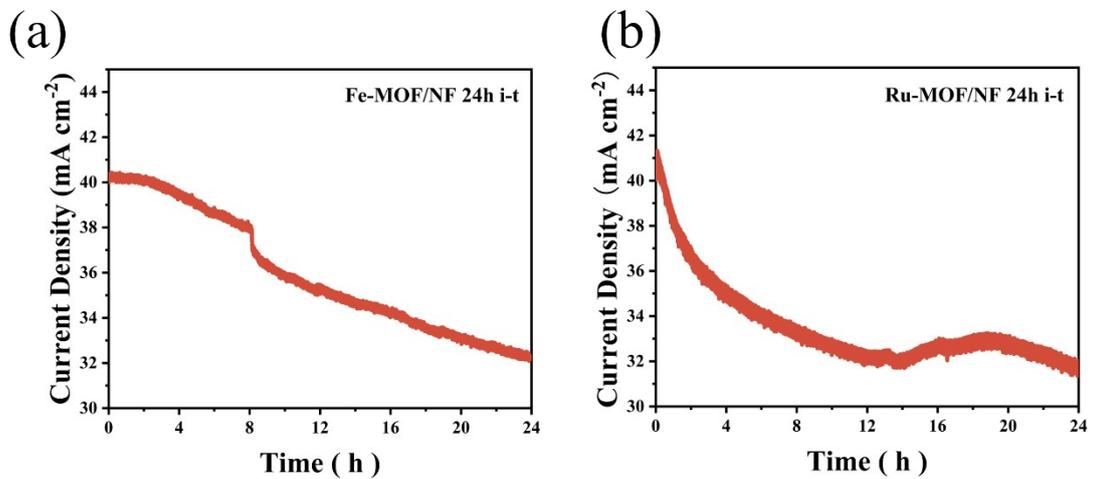
Figure S7. The chronoamperometric i-t curve of Fe-MOF /NF and Ru-MOF/NF at

40 mA cm^{-2} for 24h.
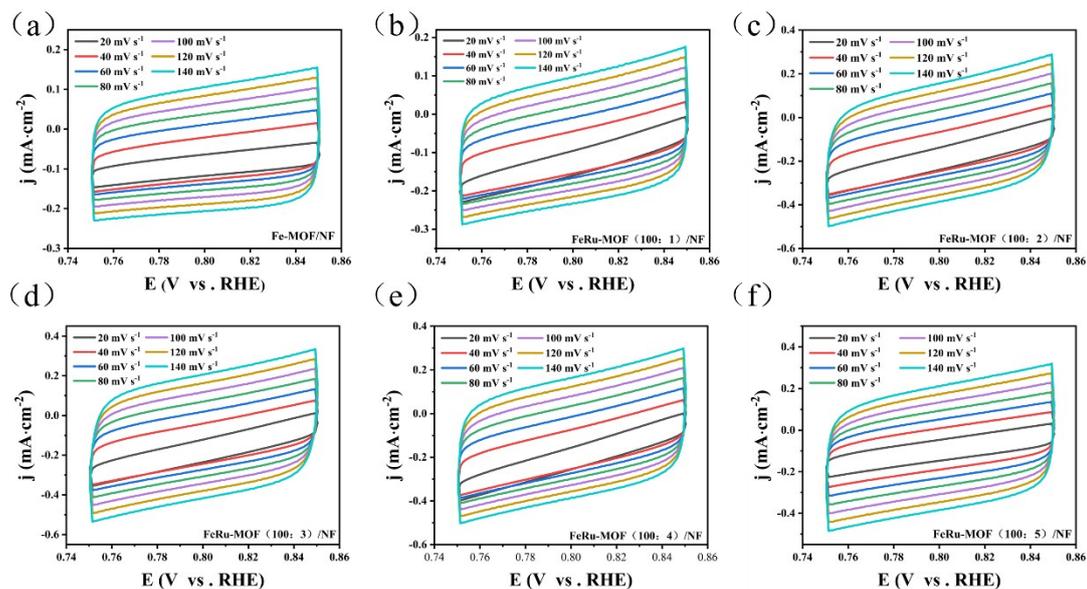
Figure S8. Electrochemical double-layer capacitance measurements of (a) Fe-MOF/NF, (b) FeRu-MOF (100:1)/NF, (c) FeRu-MOF (100:2)/NF, (d) FeRu-MOF (100:3)/NF, (e) FeRu-MOF (100:4)/NF and (f) FeRu-MOF (100:5)/NF at scan rates of 20, 40, 60, 80, 100, 120 and 140 mV s^{-1}.
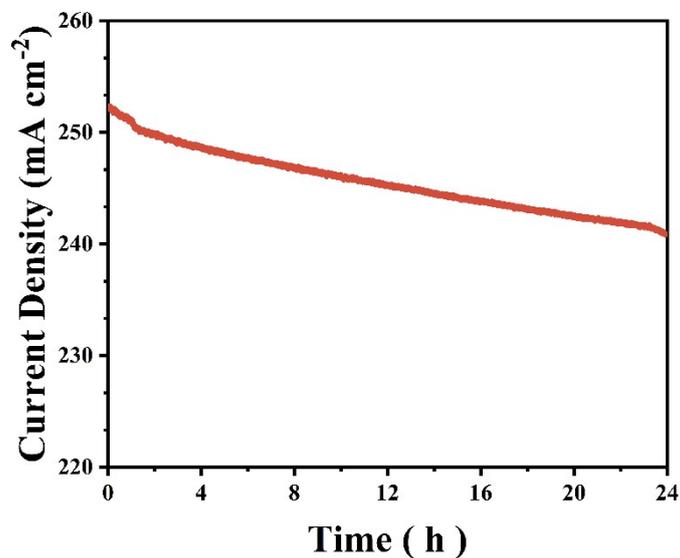
Figure S9. The chronoamperometric i-t curve of FeRu-MOF (100:3)/NF||FeRu-MOF (100:3)/NF couple at 250 mA cm^{-2} for 24h.
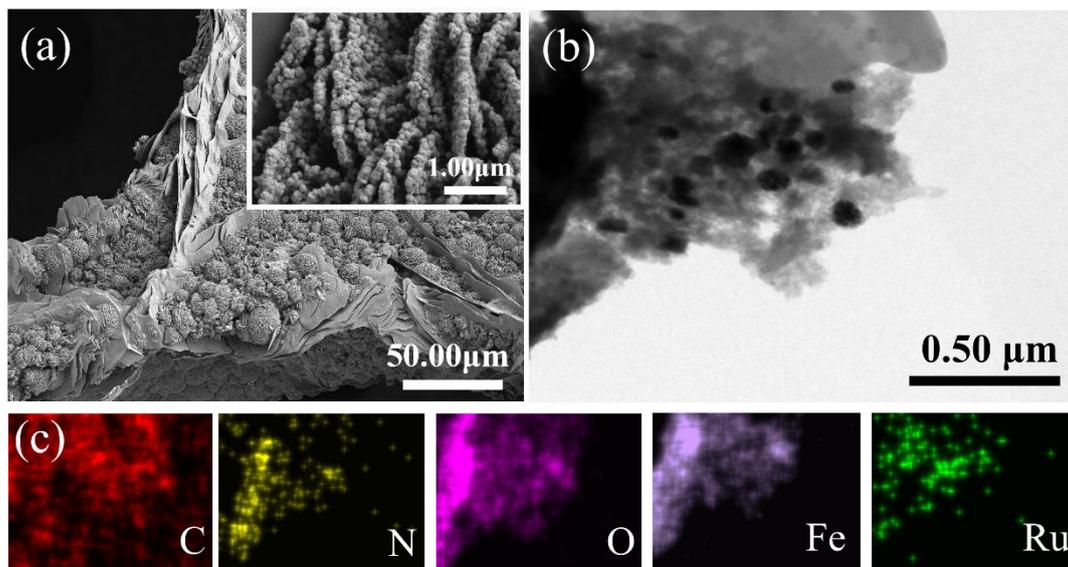
Figure S10. (a) SEM image of the post-MOR and HER FeRu-MOF (100:3)/NF. (b) TEM image and (c) elemental mapping images of the post-MOR and HER FeRu-MOF (100:3)/NF nanosheets.
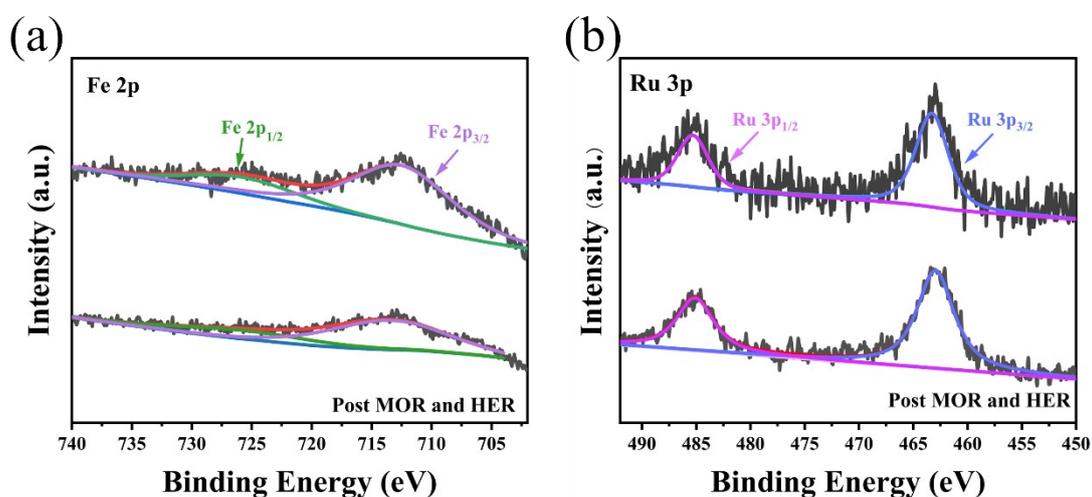
Figure S11. High-resolution (a) Fe 2p and (b) Ru 3p XPS spectra of post-MOR and HER FeRu-MOF nanosheets.

References

1. Kresse and Furthmuller, *Phys. rev.. B, Condens. matter*, 1996, **54**, 11169-11186.

2. Perdew, Burke and Ernzerhof, *Phys. Rev. Lett.*, 1996, **77**, 3865-3868.

3. *S. Grimme, J. Comput. Chem., 2006, 27, 1787-1799.*

4. J. Rossmeisl, A. Logadottir and J. K. Norskov, *Chem. Phys.*, 2005, **319**, 178-184.

5. Z. W. Seh, J. Kibsgaard, C. F. Dickens, I. B. Chorkendorff, J. K. Norskov and T.

F. Jaramillo, *Science*, 2017, **355**.

6.   V. Tripkovic, E. Skulason, S. Siahrostami, J. K. Norskov and J. Rossmeisl, *Electrochim. Acta*, 2010, **55**, 7975-7981.